Journal of Environmental Chemical Engineering 14 (2026) 121516

Contents lists available at ScienceDirect

Journal of Environmental Chemical Engineering

journal homepage: www.elsevier.com/locate/jece

Two birds with one stone: Nanostructured MWCNTs- iron-phthalocyanine/imidazolium bromide co-polymer as catalyst for both CO_2 valorization and nitro-reduction reactions

Benedetto Taormina [a,b], Francesca Cecchet [c], Michelangelo Gruttadauria [a], Carmela Aprile [b,*], Francesco Giacalone [a,*]

[a] Department of Biological, Chemical and Pharmaceutical Sciences and Technologies, University of Palermo and INSTM UdR Palermo, Viale delle Scienze, Ed. 17, Palermo 90128, Italy
[b] Laboratory of Applied Material Chemistry (CMA), Department of Chemistry, Namur Institute of Structured Matter (NISM), University of Namur, 61 rue de Bruxelles, Namur 5000, Belgium
[c] Department of Physics, Namur Institute of Structured Matter (NISM), University of Namur, 61 Rue de Bruxelles, Namur 5000, Belgium

ARTICLE INFO

Keywords:
Iron phthalocyanine
MWCNTs
CO2 valorization
Cyclic carbonates
Nitro-reduction
Amine synthesis

ABSTRACT

The straightforward synthesis of a nanostructured hybrid material in which an iron phthalocyanine/imidazolium bromide co-polymer is formed and simultaneously covalently attached to the surface of multi-walled carbon nanotubes (MWCNT) is reported. **FePC@MWCNTs**, has been characterized using different techniques such as TGA, solid state ^{13}C NMR, XPS, CHN, Raman, TEM, and physisorption. RAMAN analyses confirmed the successful covalent functionalization of the nanotubes and TEM revealed that the MWCNT were covered by the copolymer, enhancing the stability of the nanostructured hybrid material which contains 0.22 mmol/g mmol of iron phthalocyanine, as shown by combining XPS and CHN. **FePC@MWCNTs** was successfully employed as heterogeneous catalyst for two different processes: the CO_2 cycloaddition with epoxides to synthesize cyclic carbonates, in which **FePC@MWCNTs** acts as bifunctional catalyst synergistically combining Lewis acid (Fe atoms) and nucleophilic (Br^- anions) components without addition of additives (e.g. TBAB, TBAI, BMIM, etc.); and in the synthesis of arylamines through the reduction of nitro groups, which was efficiently accomplished by using microwave heating. The hybrid material demonstrated in both cases excellent catalytic activity, outperforming all the existing phthalocyanine-based systems and resulting recyclable in consecutive catalytic runs. In the CO_2/epoxide cycloaddition and the nitro-reduction reactions, no metal leaching was observed, further confirming the robustness of this material. What makes **FePC@MWCNTs** particularly noteworthy, beyond its versatility and robustness, is its simplicity and cost-effectiveness: the material is synthesized from low-cost and readily available precursors through straightforward and atom-economical methods, making it a sustainable choice and also a highly practical and cheap solution for catalysis, underscoring its potential as a valuable catalyst, and offering a sustainable alternative in an industry that often relies on more expensive and less efficient solutions. The robustness of the reported nanostructured hybrid opens the way to expanding their application in other fields such as photo-, electrocatalysis or batteries, among others.

1. Introduction

Metallo-phthalocyanines (MPCs) are a class of highly conjugated macrocyclic compounds structurally related to porphyrins, composed of four isoindole units linked via aza bridges to form a planar 18-π electron aromatic system, typically coordinated to a central metal ion. Their structure imparts remarkable thermal and chemical stability, as well as characteristic redox and photophysical properties [1]. The nature of the metal centre allows finely tuning the physicochemical features of the MPC since it plays a crucial role in processes like electron transfer, light absorption, undergoing reversible redox cycles, and eventually substrate activation for specific chemical reactions. These characteristics, along with the inherent robustness and stability of MPCs, make this class of molecules highly attractive as catalysts for a broad range of applications

* Corresponding authors.
E-mail addresses: francesca.cecchet@unamur.be (F. Cecchet), carmela.aprile@unamur.be (C. Aprile), francesco.giacalone@unipa.it (F. Giacalone).

https://doi.org/10.1016/j.jece.2026.121516
Received 2 December 2025; Received in revised form 27 January 2026; Accepted 28 January 2026
Available online 31 January 2026

[2]. Among them, electrochemical and photochemical applications are the most widespread [3,4]: indeed, the use of MPCs in processes such as CO_2 reduction [5], water splitting [6], and hydrogen production [7], whether electrochemically or photochemically driven, has been well established and continues to be the focus of extensive investigation. By contrast, the application of MPCs in thermally induced catalysis remains relatively uncommon. This is likely due to their prominent photo-electronic properties, which naturally lend themselves to the types of applications previously mentioned. Nevertheless, the exceptional stability and robustness of these molecular systems also make them well-suited for catalytic processes driven by elevated temperatures, an area that, despite its potential, remains underexplored in the current literature. However, regardless of the type of application, the use of MPCs as molecular catalyst might bring to several challenges, including their tendence to aggregate in solution, a low solubility in common solvents, and deactivation under harsh conditions. To address these limitations, a practical strategy involves immobilizing MPCs onto a support material (covalently or non- covalently), resulting in heterogeneous systems where the MPCs are more uniformly dispersed and structurally stabilized. Systems where MPCs are covalently immobilized onto the support offer several advantages over non-covalently bonded counterparts, including enhanced stability and robustness, greater resistance to thermal and mechanical stress, and a reduced risk of leaching. Various types of supports can be used for the covalent attachment of MPCs, including silica or titania [8,9], metal-organic frameworks (MOFs) [10], and, more rarely, carbon nanoforms such as single-walled carbon nanotubes (SWCNTs) and multi-walled carbon nanotubes (MWCNTs) [11]. The latter support exhibit outstanding properties, including high chemical and thermal stability, large surface area, exceptional tensile strength, and notable electrical conductivity [12,13]. A common challenge in functionalizing these types of nanomaterials with MPCs lies in the limited amount that can be covalently anchored to the surface. Recently, we reported a simple yet effective method for covalently attaching high amounts of MPCs and ionic liquid-like (IL) linkers onto the surface of MWCNTs (**MPC@MWCNTs**) [14]. The presence of the MWCNTs enhanced the catalytic performance of the resulting materials compared to unsupported analogue [15].

In this work, the straightforward synthesis of a material based on iron-phthalocyanine decorated with imidazole moieties (**FePC-Im$_4$**) and imidazolium bromide salts (**Bis-Vinyl-Imi-Br**) covalently anchored to **MWCNTs** (**FePC@MWCNT**s) has been developed. After extensive characterization using several analytical and spectroscopic techniques, its catalytic versatility and efficiency has been evaluated by testing it in two different chemical processes: the synthesis of cyclic carbonates via the cycloaddition of CO_2 to epoxides, and the synthesis of arylamines via the reduction of nitro groups. Recent studies have shown that the synthesis of cyclic carbonates via epoxide cycloaddition in the presence of CO_2 is greatly enhanced when catalyzed by a synergistic combination of a Lewis acid, which coordinates the epoxide ring to facilitate its opening, and a nucleophile, which carries out this opening [16]. For this reason, during last years, we have developed, and tested various materials where both the Lewis acid (metal cation centres such as Al, Mg, Zn, and Cu complexed in porphyrins or phthalocyanines) and the nucleophilic component (halide anions in imidazolium salts) are covalently linked in a single polymeric structure, creating diverse types of heterogeneous bifunctional materials, supported on MWCNTs [14–18].

The reduction of nitro groups to amines, on the other hand, is a well-known process [19] that has undergone numerous improvements over time. These advancements have focused on optimizing the hydrogen source, selecting suitable metal catalysts, and fine-tuning key reaction parameters such as pressure and temperature, resulting in more efficient and selective methodologies [20,21]. Currently, noble metal catalysts are predominantly used at both industrial and laboratory scales, with industrial processes typically operating at elevated temperatures up to 470 °C [22]. However, growing environmental and economic concerns have recently driven interest in more sustainable and cost-effective approaches, including the use of non-noble metal catalysts [22] and milder reaction conditions. In this regard, herein our approach employing an earth-abundant, non-toxic, and inexpensive metal such as the Fe contained in **FePC@MWCNTs**, in combination with innovative and energy-efficient techniques like microwave-assisted synthesis, represents a promising example of such sustainable strategies. Thus, the strength of this work lies in the design, synthesis, and characterization of a unique material capable of effectively catalyzing a variety of useful chemical processes of different natures.

2. Experimental section

Detailed procedures for the synthesis of precursors and materials, along with a description of the characterization techniques employed, are provided in the Supporting Information.

2.1. CO_2 conversion: catalytic experiments and recycling tests procedures

The catalytic ability of **FePC@MWCNTs** in promoting the valorization of CO_2 into cyclic carbonates was tested using a Cambridge Design Bullfrog batch reactor, featuring precise control over temperature, mechanical stirring, and internal pressure. Prior to each reaction, the catalyst was subjected to overnight drying in a vacuum oven at 60 °C to remove any adsorbed moisture. For each experiment, the selected epoxide was introduced into a PTFE vial, followed by the addition of the pre-dried catalyst under solvent-free conditions. The vial was then secured in the reactor, and the mixture was stirred at 500 rpm. To ensure an inert atmosphere, the system was purged with nitrogen for 10 min before pressurizing with CO_2 to 25 bar. The reaction mixture was then heated to the target temperature at a controlled ramp of 5 °C/min and maintained at that temperature throughout the reaction to optimize conversion. Once the reaction was complete, the reactor was cooled to room temperature and depressurized. The catalyst was separated from the product mixture via filtration through a 0.45 μm Millipore membrane. The resulting filtrate was analyzed by ^{1}H NMR in $(CD_3)_2SO$ to determine product composition. Recyclability of the catalyst was assessed by repeating the same reaction conditions over multiple cycles. After each run, the catalyst was recovered by filtration using a 0.45 μm membrane and then subjected to thorough washing: three times with 50 mL portions of toluene, three times with 50 mL portions of ethanol, and once with diethyl ether. The washed catalyst was dried overnight at 60 °C in a vacuum oven before reusing, while carefully maintaining the same catalyst-to-epoxide molar ratio for all successive cycles to ensure reproducibility. Inductively Coupled Plasma - Optical Emission Spectrometry (ICP-OES) analysis has been carried out on the crude reaction mixtures of the recycling tests, showing that negligible Fe-leaching took place (0.13–0.26 ppm range per cycle).

2.2. NO_2 reduction: catalytic experiments and recycling tests procedures

The catalytic ability of **FePC@MWCNTs** in promoting the reduction of nitro-groups (-NO_2) to amino groups (-NH_2) was tested by dissolving 0.5 mmol of the nitro-substrate together with two equivalents of hydrazine hydrate ($N_2H_4{\cdot}H_2O$) in 0.5 mL of ethylene glycol. To this solution, 5 mg of the catalyst was added, and the mixture was homogenized through sonication for 3 min. The reaction vessel was then sealed and heated to 100 °C for 30 min using a CEM DISCOVER mono-mode microwave system set at 80 W. Reaction progress was periodically monitored using thin-layer chromatography (TLC) with variable ratios of ethyl acetate and hexane as the eluent. Upon completion, the reaction mixture was transferred to a separation funnel with the addition of 20 mL of water and 20 mL of dichloromethane, ensuring that all material, including the catalyst, was fully recovered from the vessel. The organic phase was collected, and the aqueous layer was extracted twice more with 20 mL portions of dichloromethane. The combined organic extracts were dried over anhydrous $MgSO_4$, filtered, and purified by

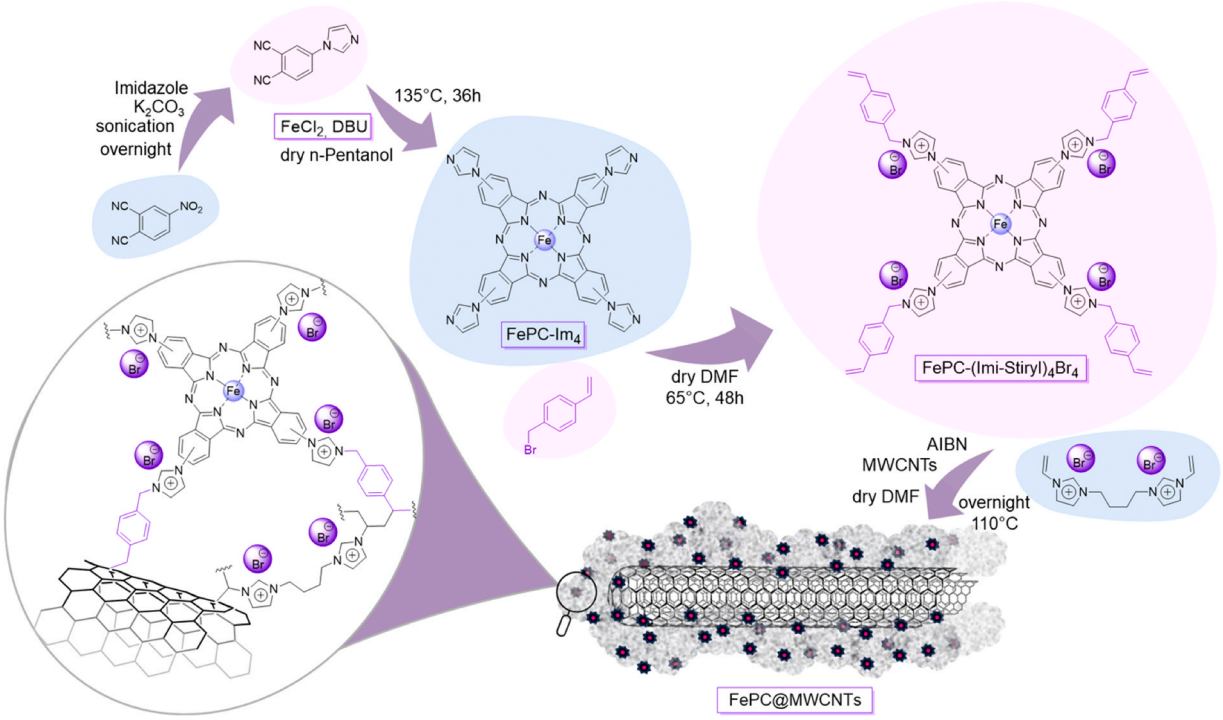

Scheme 1. Chemical pathway for the preparation of **FePC@MWCNTs.**

flash column chromatography (using ethyl acetate:hexane in variable ratios) to afford the desired product. For catalyst recycling experiments, 1 mmol of 4-nitrobenzonitrile was employed under identical reaction conditions. TLC (ethyl acetate:hexane = 1:2) was used to confirm product formation. During separation, the catalyst remained in the aqueous phase, which was transferred into a 45 mL Falcon tube and supplemented with 20 mL of acetone. The tube was centrifuged to collect the catalyst as a solid pellet, which was then washed sequentially with 40 mL of methanol and acetone. The recovered catalyst was dried at 60 °C for 1 h and reused in subsequent reaction cycles, maintaining consistent catalyst-to-substrate ratios to ensure reproducibility. The combined organic layers were dried over $MgSO_4$, filtered, and subjected to flash column chromatography (ethyl acetate:hexane = 1:4) to isolate the purified product.

3. Results and discussion

The synthesis of the iron phthalocyanine with four peripheral imidazole moieties (**FePc-Im$_4$**) was carried out following synthetic depicted in Scheme 1: firstly 4-nitrophthalonitrile has been converted into 4-(1*H*-imidazol-1-yl)phthalonitrile, which was in turn used as building block to form **FePC-Im$_4$** –a mixture of four regioisomers– through a templated synthesis where $FeCl_2$ acts as a templating agent. Mass spectrometry confirmed the successful synthesis of **FePC-Im$_4$** (Figure S1), while UV-Vis Spectroscopy revealed the characteristic spectrum of metal phthalocyanines (Figure S2): the Soret band (B band, 300–400 nm), attributed to π–π* electronic transitions within the conjugated phthalocyanine structure, is clearly observable. In addition, the Q band (600–750 nm), a hallmark of metalated phthalocyanines, is prominently present and split into two distinct peaks since all the isomers of **FePC-Im$_4$** are asymmetric [23]. Hence, **FePC-Im$_4$** underwent a nucleophilic substitution with 4-benzylvinyl bromide to quaternize the imidazole moieties and give the corresponding **FePC-(Imi-Styryl)$_4$Br$_4$**. This quaternization into imidazolium bromide has been confirmed and quantified *via* Fourier transform-infrared (FT-IR) spectroscopy and X-ray photoelectron spectroscopy (XPS). Comparing the IR spectra of **FePC-Im$_4$** and **FePC-(Imi-Styryl)$_4$Br$_4$** reveals key differences (Figure S3): despite overnight drying at 60°C, the spectrum of **FePC-(Imi-Styryl)$_4$Br$_4$** shows an intense band at 3200–3600 cm^{-1} , indicating O-H stretching from adsorbed water. This is ascribed to the highly hygroscopic nature of the newly formed imidazolium salt groups in the molecule. Another band in this spectrum is ranging from 2700 to 3100 cm^{-1} , and it is attributed to the stretching vibrations of C–H bonds from both the aromatic and aliphatic carbon atoms in the newly incorporated styryl groups [24–28]. Additionally, the stretching vibration bands of the C═C and C═N bonds within the aromatic core of the phthalocyanine appear between 1480 and 1640 cm^{-1} , overlapping with the bands associated with the stretching vibrations of the vinyl C═CH_2 double bond present in **FePC-(Imi-Styryl)$_4$Br$_4$** [24–28]. XPS analysis (Figure S4) confirmed the presence of bromine, revealing a strong peak around 68 eV, deconvoluted into the characteristic Br $3d_{3/2}$ and Br $3d_{5/2}$ signals. This analysis also enabled the estimation of the quaternization degree of the imidazole fractions: the high-resolution XPS spectrum of the N1s region for **FePC-(Imi-Styryl)$_4$Br$_4$** (Figure S4) displays two distinct contributions at 398 eV and 402 eV. The former corresponds to nitrogen within the phthalocyanine core, while the latter originates from nitrogen in the imidazole rings [15]. The area under the curve (A. U.C.) of these signals allows quantifying a 1:1 ratio *circa*, thus confirming the successful complete quaternization of all four imidazole groups into imidazolium bromide fractions. Once characterized, **FePC-(Imi-Styryl)$_4$Br$_4$** was then co-polymerized in dry DMF with **Bis-Vinyl-Imi-Br** in the presence of MWCNTs using an atom-economical radical polymerization process initiated by AIBN to produce **FePC@MWCNTs** in a high mass yield of 82 % (Scheme 1). The role of MWNCTs is triple: 1) acting as a templating agent in order to obtain a nanostructured material; 2) enhancing the surface area of the cross-linked polymer resulting in a major number of accessible catalytic sites; 3) producing a more robust material.

The same synthetic approach described here above has been used for the preparation of the unsupported catalyst **FePC-SIBI-Br**, that is without using MWCNTs during the polymerization process [15]. **FePC-SIBI-Br** has been synthesized with the only aim to make some Raman investigations that will be further discussed.

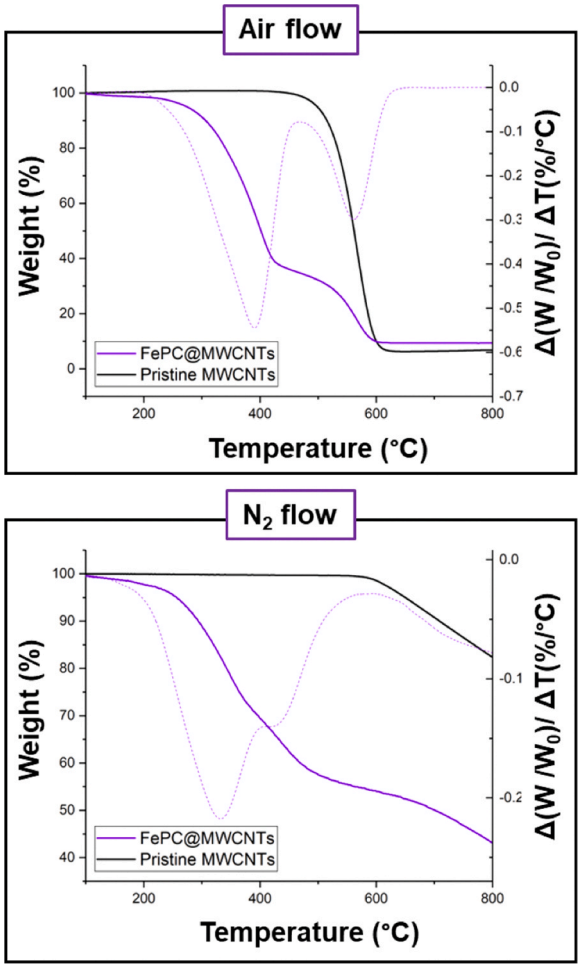

Fig. 1. Thermogravimetric analyses (TGA, plain lines) and differential thermogravimetric analyses (DTG, dotted lines) graphs obtained for **FePC@MWCNTs** in air flow and N_2 flow.

3.1. *Characterization of FePC@MWCNTs*

Thermogravimetric analysis (TGA) was performed under both air and nitrogen flow for **FePC@MWCNTs** (Fig. 1): despite the two graphs showed different degradation profiles, due to the presence or lack of oxygen during the thermal analysis, however, regardless of the gas flow used, the material exhibited remarkable thermal stability during the heating ramp, with the first signs of degradation appearing only above 300°C in both cases.

Solid-state cross-polarization magic angle spinning ^{13}C NMR spectroscopy (ss CP-MAS-^{13}C NMR), employing a total suppression of spinning sidebands (TOSS) pulse sequence, was performed on **FePc@MWCNTs** (Figure S5). The resulting spectrum exhibited a low signal-to-noise ratio and notably broad signals, primarily due to the ferromagnetic nature of the iron centers in the phthalocyanine moieties. These ferromagnetic centers significantly enhance nuclear relaxation, particularly the spin–spin relaxation time (T_2), thereby compromising spectral resolution and complicating the analysis. Despite these limitations, two distinct groups of signals have been discerned. The first, appearing in the 120–150 ppm range, corresponds to the aromatic carbon atoms of the phthalocyanine, imidazolium, and phenyl ring systems. The second group, located between 25–60 ppm, is attributed to aliphatic carbon atoms of the material. Overall, this is a set of signals quite consistent with those we have observed in similar materials [14].

The XPS survey spectrum of **FePC@MWCNTs** (Fig. 2) confirmed the presence of all expected elements. The high-resolution Fe 2p spectrum displayed the characteristic Fe $2p_{1/2}$ and Fe $2p_{3/2}$ doublet together with its satellite peaks at 724 eV and 710.4 eV, respectively, indicating that the metal is in the Fe^{2+} oxidation state (the same peaks were also found for the precursor **FePC-(Imi-Styryl)$_4$Br$_4$**, see Figure S4) [29]. Similarly to **FePC-(Imi-Styryl)$_4$Br$_4$**, the high-resolution XPS spectrum of the N1s region (Fig. 4) revealed two distinct nitrogen contributions, corresponding to the different nitrogen types in this material: the nitrogen signal from phthalocyanine cores appeared at 398.5 eV, with an A.U.C. of 25 %, while the imidazolium-related nitrogen signal was found at 401.5 eV, accounting for 75 % A.U.C. The ratio N_{imi}/N_{PC}= 3 (nitrogen atoms in imidazolium rings/nitrogen atoms in phthalocyanine rings), calculated from these XPS outcomes, is fully consistent with the molar amounts of **FePC-(Imi-Styryl)$_4$Br$_4$** and **Bis-Vinyl-Imi-Br** used for the preparation of the material (Scheme 1). These XPS results have been combined with those of CHN elemental analysis to calculate the metal loading of **FePC@MWCNTs** (Table S1), which resulted equal to 0.22 mmol/g.

The covalent functionalization of the co-polymer on MWCNTs surface was also confirmed by Raman spectroscopy. Fig. 3 shows two sets of Raman data. Fig. 3**a-f**, on the left, shows the Raman spectra of the different materials and precursors, namely **FePC@MWCNTs** (Fig. 3**a**), the unsupported co-polymer **FePC-SIBI-Br** (Fig. 3**b-c**), **FePC-(Imi-Styryl)$_4$Br$_4$** (Fig. 3**d**), **FePC-Im$_4$** (Fig. 3**e**) and **Bis-Vinyl-Imi-Br** (Fig. 3**f**). Fig. 3**g-j**, on the right, shows the Raman spectra of the targeted catalyst **FePC@MWCNTs** as a function of the laser power energy (1.4–14 mW range) as well as the spectra of the pristine MWCNTs (Fig. 3**k**). The spectra of Fig. 3**a-f** revealed that the distinctive peaks of the monomeric components were observable both in the spectrum of the supported material **FePC@MWCNTs** acquired at 1.4 mW (Fig. 3**a**) and in the spectrum of the non-supported material **FePC-SIBI-Br** acquired at o.45 mW (Fig. 3**c**), albeit with slight broadening of the signals, as a result of the amorphous character of polymers (for more details regarding the vibration bands see Table S2). Notably, the absence of the intense vinyl stretching vibrations bands at 1650 cm^{-1} found in **Bis-Vinyl-Imi-Br** (Fig. 3**f**), and the further appearance of new peaks at 1600–1620 cm^{-1} in the polymerized materials indicate the success of the radical polymerization, where the vinyl bonds have randomly formed new C–C covalent bonds both among themselves and with the surface Csp^2 atoms of the MWCNTs.

In addition to the validation of the covalent functionalization of the co-polymer on the MWCNTs, another important result revealed by the Raman analysis has been obtained with investigating the effects of the laser energy on the Raman responses of supported and unsupported materials. Indeed, the laser energy required to record the spectrum of the unsupported copolymer **FePC-SIBI-Br** should not have exceeded 0.45 mW (Fig. 3**b**), otherwise the sample would have burned, producing a Raman spectrum with broad and poorly defined contributions (Fig. 3**c**). Instead, in the case of **FePC@MWCNTs**, it was possible to increase the laser energy up to 1.4 mW (Fig. 3**g**) without noticing differences in the spectral features (compare Fig. 3**a** and Fig. 3**g**), which is a proof that there has been no degradation. To investigate whether the presence of nanotubes was in charge of the increased resistance of the material to the higher-energy stimuli, both accumulation and single-point Raman measurements were carried out on **FePC@MWCNTs** and **FePC-SIBI-Br**. In the accumulation mode, multiple Raman spectra were subsequently recorded on the same point of the sample with gradually increasing the laser power, while in the single-point mode, a fresh spot of the sample was used to acquire a new spectrum directly with the desired laser power. In the accumulation mode, the Raman spectra showed progressive changes in the spectral features, indicating that the sample was beginning to degrade- an effect known as accumulation damage-. It was found that **FePC-SIBI-Br** showed accumulation effects starting from 0.45 mW. In single-point mode, the sample was damaged when the laser power exceeded the range of 0.45–0.54 mW. Interestingly, **FePC@MWCNTs** began to show accumulation damages only once the range was set to between 0.9–1.4 mW. In single-point mode, the

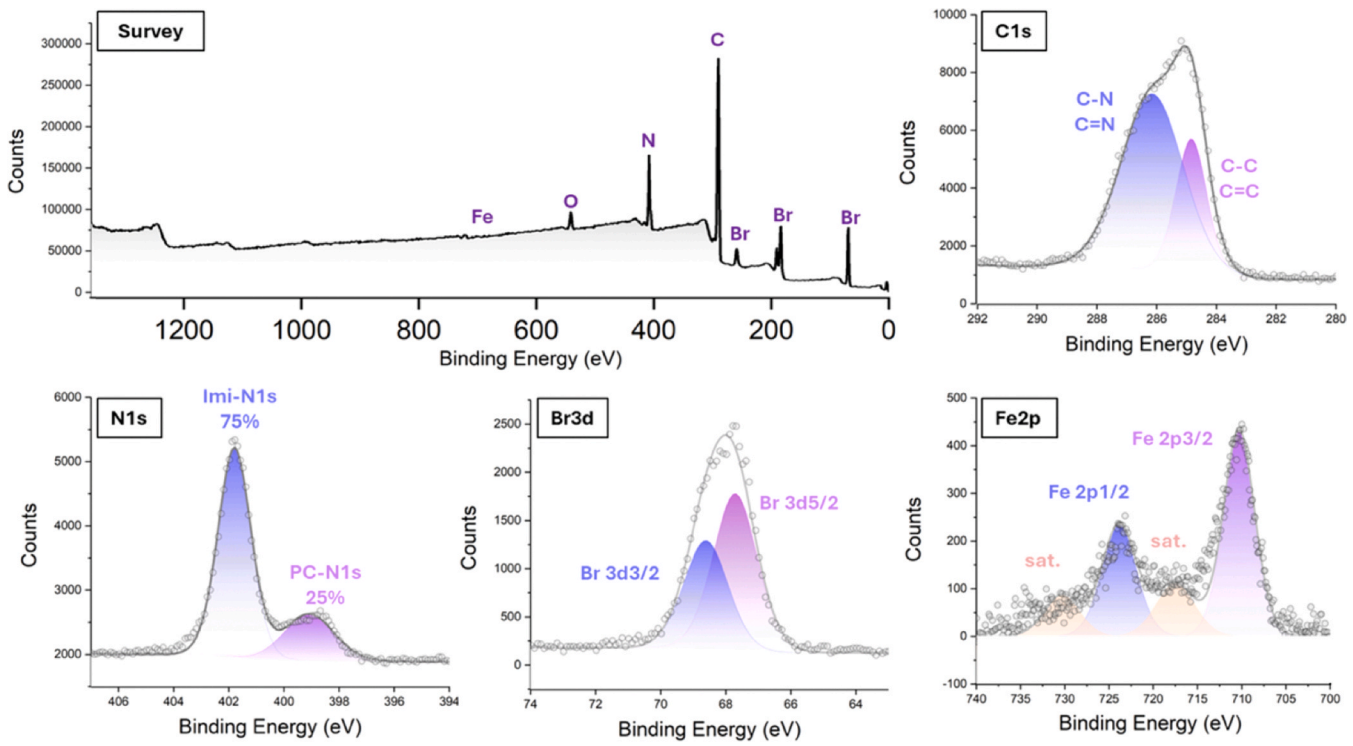

Fig. 2. XPS survey and high resolution of the C1s, N1s, Br3d and Fe2p regions spectra of **FePC@MWCNTs**.

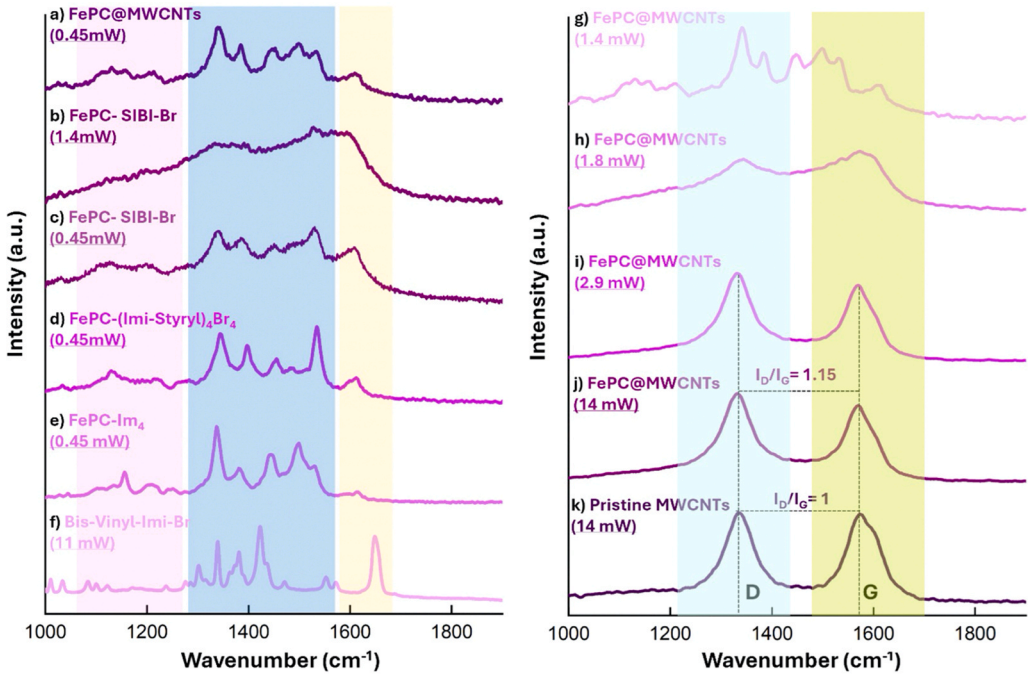

Fig. 3. On the left Raman spectra at 532 nm of (a) **FePC@MWCNTs** acquired at 0.45 mW, (b-c) **FePC-SIBI-Br** acquired at 1.4 mW and 0.45 mW, respectively; (d) **FePC-(Imi-Styryl)$_4$Br$_4$** acquired at 0.45 mW; (e) **FePC-Im$_4$** acquired at 0.45 mW; (f) **Bis-Vinyl-Imi-Br** acquired at 11 mW. On the right Raman spectra at 532 nm of (g-j) **FePC@MWCNTs** acquired at 1.4 mW, 1.8 mW, 2.9 mW and 14 mW, respectively; (k) **pristine MWCNTs** acquired at 14 mW.

sample only degraded when the laser power exceeded 1.4 mW. This behavior undoubtedly demonstrated that the supported **FePC@MWCNTs** owns a higher resistance to the laser power than the unsupported **FePC-SIBI-Br**. This notable result, together with the ones of TGA analysis previously discussed (Fig. 1), underscores the exceptional stability and thermal resistance of **FePc@MWCNTs**. To obtain further insight into the resistance of **FePc@MWCNTs** to the laser power, the second dataset presents the Raman spectra of **FePC@MWCNTs** (Figs. 3**g**-3**j**) at increasing laser energies, which are compared with the spectrum of pristine MWCNTs acquired at 14 mW (Fig. 3**k**). As soon as the energy increased from 1.4 mW to 1.8 mW(Figs. 3**g**-3**h**), co-polymer-related peaks disappeared, leaving only the characteristic D and G bands of MWCNTs (Fig. 3**k**). The D band is known to come from defects in the nanotube lattice, and it is usually associate to the presence of Csp^3

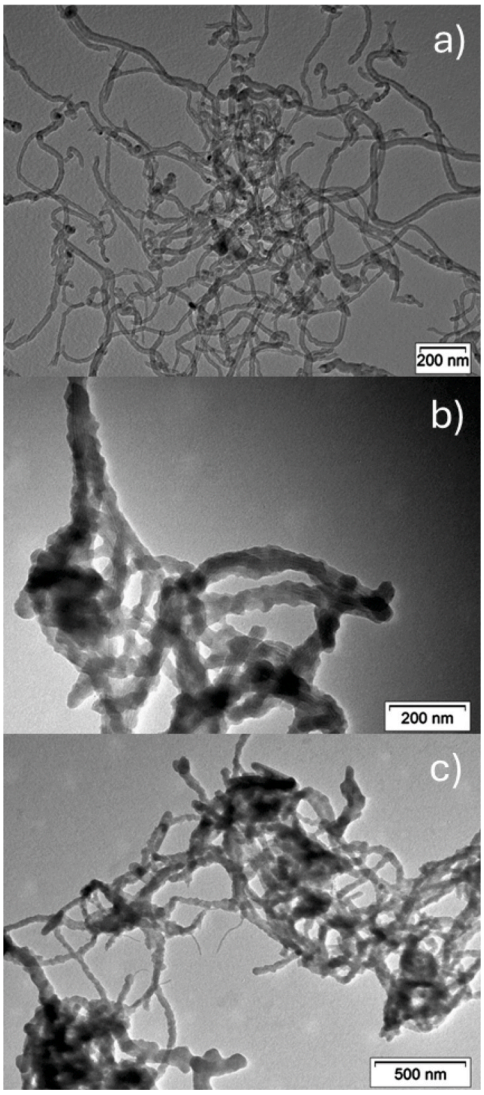

Fig. 4. TEM micrographs of (a) pristine MWCNTs, and (b,c) **FePC@MWCNTs**.

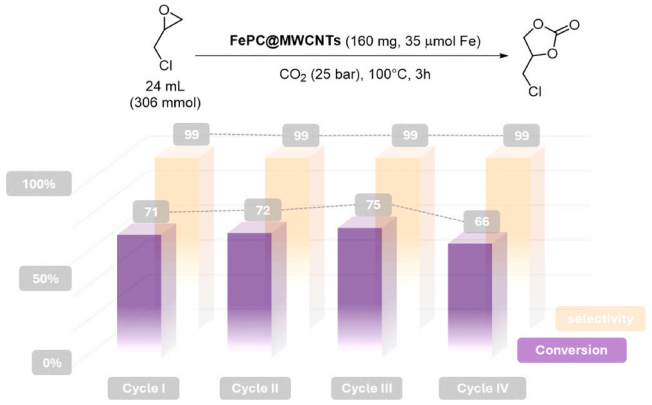

Fig. 5. Conversion and selectivity value of the synthesis of 4-(chloromethyl)-1,3-dioxolan-2-one via cycloaddition of epichlorohydrin and CO_2 catalyzed by **FePC@MWCNTs** in four catalytic cycles where the catalyst has been recycled each time. Conversions have been calculated via ^{1}H NMR analysis (Fig. S7-S10). TON values have been calculated as moles of product obtained/ mole of active sites (Fe or Br^-), while TOF have been calculated as TON/ reaction time (Table S3).

atoms, while the G band reflects carbon symmetric vibrational modes along the nanotube surface, and it is associated to the Csp^2 network [30]. The ratio of D to G peak intensities (I_D/I_G) serves as a key indicator of surface disorder, as covalent functionalization of the MWCNTs surface for instance [30]. The I_D/I_G ratio of 1.15 for the **FePC@MWCNTs** acquired at 2.9 mW and 14 mW (Figs. 3**i**-3**j**) compared to I_{D0}/I_{G0} ratio of 1 for pristine MWCNTs (Fig. 3**k**) indicated a higher content of defects on the nanotube surface in the former, as expected following the covalent functionalization arising from the polymerization on the nanotube surface (Scheme 1). The Raman spectra outlined that the laser power degraded the copolymer layer wrapped around the surface of the MWCNTs, ultimately exposing the now defect-richer surface.

Transmission Electronic Microscopy (TEM) allowed to acquire insight on the morphology of **FePC@MWCNTs** in comparison with pristine MWCNTs (Fig. 4): the final hybrid material appears as nanosturctured assembly, where the **FePC-(Imi-Styryl)$_4$Br$_4$** and **Bis-Vinyl-Imi-Br** based co-polymer uniformly coats the nanotube surface, leaving only few exposed nanotube tips. Once again, despite the random nature of the copolymerization process between two monomers endowed with multiple polymerizable double bonds, the electron-rich nanotubes act as a template for the growth of the highly crosslinked electron poor imidazolium network likely through π–π interactions, as previously observed by us in other poly-imidazolium systems [14,17,31–35]. Finally, N_2 physisorption measurement was employed to evaluate the specific surface area (S.S.A.) of **FePC@MWCNTs** which resulted of c.a. 70 m^2/g, notably lower than that of pristine MWCNTs (240 m^2/g). This reduction was expected, as the polymerization process extensively engaged the nanotube surface during material synthesis.

3.2. *Cycloaddition of epoxides and CO_2 catalyzed by FePC@MWCNTs*

FePC@MWCNTs was tested as bifunctional catalyst for the conversion of epichlorohydrin into the corresponding cyclic carbonate 4-(chloromethyl)-1,3-dioxolan-2-one *via* cycloaddition with CO_2 without the need of adding any additive. The catalyst resulted extremely active in just 0.01 mol% (based on Fe), achieving high conversion and being recyclable at least four times, with only a slight decrease in efficiency during the final cycle (Fig. 5). In our earlier studies on these bifunctional materials [14–18], we have already highlighted the significant role played by the synergistic interaction between a Lewis acid and a nucleophile in enhancing the cycloaddition of CO_2 and epoxides to form cyclic carbonates (Figure S6): in this process, the epoxide first coordinates to the metal cation (Lewis acid), which boosts its reactivity toward nucleophilic attack by the bromide ion (nucleophile, Figure S6a). This leads to the formation of a first alkoxide intermediate, which subsequently reacts with CO_2 to generate a second anionic intermediate (Figure S6b). Finally, the closure of this latter gives rise to the formation of the cyclic carbonate, accompanied by the release of the bromide ion (Figure S6c). Notably, a blank experiment conducted using only MWCNTs (160 mg) as the catalyst (reaction conditions: epichlorohydrin, 306 mmol, 100 °C, 3 h; CO_2 25 bar, 500 rpm) showed no detectable conversion. XPS spectroscopy and CHN elemental analysis, carried out on **FePC@MWCNTs** after the fourth catalytic cycle with epichlorohydrin (Figure S11a and Table S1), were combined to estimate a Fe loading of 0.19 $mmol_{Fe}/g$, which is very close to the initial value of 0.22 mmol/g estimated for the fresh material. This finding is in strict agreement with our previous studies [14] and is confirmed by ICP-OES since minimal Fe leaching during recycling has been found (0–13–0.26 ppm per cycle). Interestingly, the thermogram of the used catalyst displays the same shape of the fresh one with the same degradation processes (Figure S11b), once again highlighting the robustness of the material.

To further assess the catalytic efficiency of **FePC@MWCNTs** in the synthesis of cyclic carbonates, the catalyst was tested with four different epoxides (Table 1). In comparison to other metal-phthalocyanine-based bicomponent catalytic or bifunctional systems (see Table S4) [14,15,

Table 1
Conversion of different epoxydic substrates into their corresponding cyclic carbonate catalysed by **FePC@MWCNTs**.

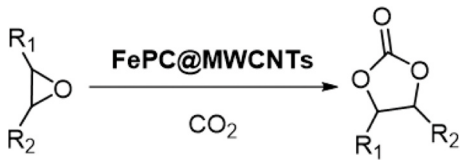

Entry	Substrate	Temperature (°C)	time (h)	Conversion (%)	Selectivity (%)[a]	TON[b]	TOF (h^{-1})[b]
1[c]	 OH 360 mmol	80	3	50	>99	16,360	5,450
2[d]	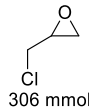 Cl 306 mmol	100	3	75	>99	6,560	2,190
3[e]	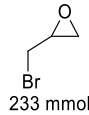 Br 233 mmol	100	3	60	>99	6,350	2,120
4[f]	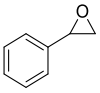 210 mmol	125	24	58	>99	11,100	460

a) Selectivity towards the corresponding cyclic carbonate; b) values calculated towards the amount of Fe in the catalyst, to see TON and TOF values towards the nucleophile Br^- see Table S3. Conversion values have been estimated via ^1H NMR (Figure S12-S15); c) 24 mL of epoxide (360 mmol), 50 mg cat. (11 μmol of Fe), CO_2 25 bar; d) 24 mL of epoxide (306 mmol), 160 mg cat. (35 μmol of Fe), CO_2 25 bar; note that this entry corresponds to the third catalytic cycle test of the previous dataset e) 20 mL of epoxide (233 mmol), 100 mg cat. (22 μmol of Fe), CO_2 25 bar; f) 24 mL of epoxide (210 mmol), 50 mg cat. (11 μmol of Fe), pCO_2 25 bar.

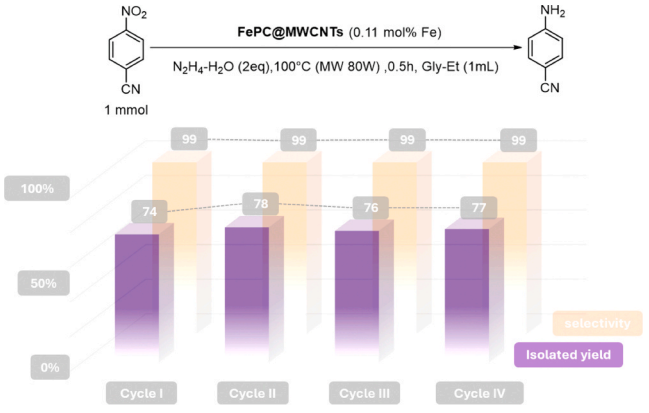

Fig. 6. Isolated yield and selectivity values for the synthesis of 4-aminobenzonitrile via nitro-reduction of 4-nitrobenzonitrile catalyzed by **FePC@MWCNTs** in four different catalytic cycles where the catalyst has been recycled each time. Isolated yields have been estimated basing on the amount of product recovered after the flash column purification, assuring the purity of the sample via ^1H NMR analysis (Fig. S22-S25). TON values have been calculated as moles of product obtained/ mole of active sites (Fe), while TOF have been calculated as TON/ reaction time (Table S5).

36–41], **FePC@MWCNTs** resulted the most active one, both in terms of TON and TOF, even with respect to those examples in which metal-phthalocyanine were used in homogeneous catalysis [36,37]. **FePC@MWCNTs** proved indeed to be particularly effective in converting significant amounts of glycidol in a short time, with a loading as low as 0.003 mol%, thus achieving remarkable TON and TOF values of 16,360 and 5,450 h^{-1}, respectively (Table 1, entry 1). **FePC@MWCNTs** was efficient in reaching high conversions also when epoxides containing halogens, such as epichlorohydrin and epibromohydrin, were employed (Table 1, entries 2 and 3). Finally, also styrene oxide gave very good results with the use of just 0.005 mol% of catalyst (Table 1, entry 4). Interestingly, the catalytic performance displayed by **FePC@MWCNTs** are among the best reported for heterogeneous bifunctional systems [42–46].

It is worth to note that, although the reaction conditions used here (80–125 °C, 25 bar of CO_2) may appear as not mild, it must be considered that large quantities of epoxide are used (>200 mmol, >20 mL). On the contrary, using just one equivalent of CO_2 at atmospheric pressure would require a reactor of almost 5 L at room temperature. Reducing the size and/or the volume of all the process plant components represents one of the goals of the process intensification [47] and, in this regard, high CO_2 pressures make possible to considerably abate the reactor volume. Finally, as a practical example, the industrial production of propylene carbonate can be carried out within a reactor operating at 20 bar and 180 °C in the presence of a homogeneous catalyst [48], in a similar way to those here reported, meaning that only modest changes would be required to adapt the cyclic carbonate preparation described here on a large scale.

3.3. *Reduction of nitro-groups to amine catalyzed by FePC@MWCNTs*

FePC@MWCNTs has been employed as catalyst to promote the synthesis of amines *via* the reduction of nitro-groups. The mechanism of this nitro-reduction process is not yet fully understood; however, several hypotheses have been proposed, supported by studies with extensive

Table 2
Screening tests of the nitro-reduction process operated by **FePC@MWCNTs** as catalyst for different kinds of nitro-substrate.

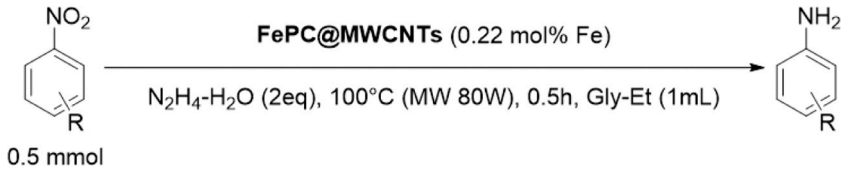

Entry	substrate	Isolated yield (%)	TON[a]	TOF[b]
1	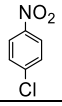	91	420	840
2	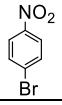	94	430	860
3	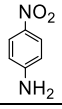	99	450	900
4[c]	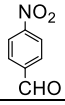	82	370	740
5	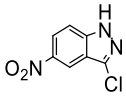	94	420	840
6		67	320	640
7		93	420	840
8	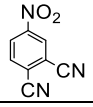	85	390	780

Isolated yields have been estimated based on the amount of product recovered after the flash column purification, assuring the purity of the sample via ^{1}H NMR analysis (Figure S26-S33). a) TON = (mol of product)/(mol of metal in the catalyst used to obtain that product); b) TOF= TON/ reaction time; c) isolated as hydrazone species.

instrumental backing (Figure S16) [49]. After several trials and attempts, hydrazine monohydrate has been used as reducing agent of choice, ethylene glycol as solvent, 4-nitrobenzonitrile as benchmark substrate for recycling tests, at an operative temperature of 100°C. The heating mode has been also carefully evaluated. In particular, the use of microwaves compared to a traditional heating plate has proven to be highly advantageous: indeed, using a standard heating plate at 100°C, with 0.1 mol_{Fe}% of catalyst and a reaction time of 3 h gave rise to a total conversion of 4-nitrobenzonitrile into the targeted product of approximately 77 % (Figure S17), which could be increased to 90 % (Figure S18) using an extended reaction time of 24 h, while keeping all other conditions constant. Instead, microwave heating drastically enhanced the process efficiency, especially in terms of reaction time, with achieving a total and selective conversion of 80 % sin only 0.5 h (Figure S19). This condition not only improved the reaction performance but also enhanced the sustainability of the catalytic process thanks to the significant reduction in energy consumption. A blank test without catalyst was performed under the above reaction conditions: this latter produced only 10 % of isolated yield, with also traces of other compounds, which were difficult to separate from the main product though clearly visible in the ^{1}H NMR spectrum (Figure S20). It was also observed that extending the reaction time to 1 h (still without using a catalyst) using microwaves not only did not improve the yield, but also it led to the formation of numerous stable intermediates and other by-products, making useless trying to isolate the targeted one (Figure S21). This result further confirmed that the catalyst played an essential role in achieving good yields in the process. The tests here above highlighted that **FePC@MWCNTs** succeeded in acting as catalyst to promote the reduction of 4-nitrobenzonitrile to 4-aminobenzonitrile at the given conditions (Fig. 6), demonstrating to be recyclable for at least four cycles.

In order to evaluate more thoroughly the effectiveness of **FePC@MWCNTs** in promoting nitro-reduction to amines, additional tests were conducted using different nitro-derivatives (Table 2). Under the operating conditions used, **FePC@MWCNTs** proved to be a highly versatile catalyst, leading to the production of very high isolated yields of the corresponding amine for almost all the substrates tested. It is difficult to compare the results obtained from **FePC@MWCNTs** in the nitro-reduction with those obtained from other reported systems. This difficulty mainly arises from the fact that at least one or more parameters or conditions, such as the substrate, the reducing agent, the solvent, the metal used as catalyst, and the support for the metal, differ from our

system. Hence, we decided to compare our results with those from other studies in which metal-phthalocyanines have been used for nitro-reductions (see Table S5) [49–52]: given its low loading, although **FePC@MWCNTs** did not always achieve better yields than the other catalytic systems in exam, when considering the TON and TOF values, however it clearly stands out as the most active and competitive catalyst among the evaluated homogeneous catalytic systems, both for performance and versatility. The robustness and catalytic activity of **FePC@MWCNTs** outperforms several other different catalytic systems employing hydrazine hydrate as reductant [53–56].

4. Conclusions

The present study reports the synthesis of a nanostructured hybrid nanomaterial comprising an iron phthalocyanine tetraimidazolium bromide and an organic linker containing imidazolium bromides, which are co-polymerized onto the surface of multi-walled carbon nanotubes. Here the electron-rich MWCNTs act as a template for the controlled growth of the crosslinked electron poor imidazolium network through π−π interactions. The targeted material **FePC@MWCNTs** underwent a deep characterization based on different analytical tools, such as XPS, TEM, FT-IR, Raman, CHN, N_2 physisorption, and TGA. In particular, Raman analyses provided valuable insights into the covalent functionalization of the copolymer on the nanotube surface, as well as into how the presence of MWCNTs reinforced the stability of **FePC@MWCNTs** compared to the non-supported counterpart **FePC-SIBI-Br**. After its comprehensive characterization, **FePC@MWCNTs** was successfully tested in promoting the synthesis of cyclic carbonates through the cycloaddition of epoxides and CO_2 without the need of additives, proving to be particularly active and recyclable in the case of epichlorohydrin and glycerol, especially when compared to other systems used for the same purpose (Fig. 5, Table 1, Table S3). Seeking further applications for this material, we demonstrated that **FePC@MWCNTs** also acts as a highly efficient, robust, and recyclable catalyst in the synthesis of amines *via* the reduction of nitro groups. In this context, the application of microwaves has proven to remarkably boost this process if compared to a traditional heating system. Notably, based on its TON and TOF values, **FePC@MWCNTs** outperforms many metal-phthalocyanine-based catalysts reported in the literature (Fig. 6, Table 2, Table S4). In addition, the robustness of this material was demonstrated by ICP analyses performed on the reaction mixtures collected after each catalytic recycling run, which revealed only trace amounts of Fe (0.13–0.26 ppm per cycle). Consistently, CHN and XPS analyses (Table S1, Figure S11) showed that the elemental composition of **FePC@MWCNTs** did not undergo significant changes, leading to the estimation of a metal content of 0.19 $mmol_{Fe}/g_{material}$, which is very close to the initial value of 0.22 $mmol_{Fe}/g_{material}$. Overall, these findings confirm the high stability of the catalyst and the negligible extent of Fe leaching throughout the recycling experiments. In conclusion, this study gives a highly promising, versatile, and sustainable work perspective, because in a landscape that produces many catalysts for the same process, on the contrary here it has been demonstrated that the same catalyst can be exploited for multiple processes. The robustness and versatility of the reported bifunctional nanostructured hybrid, in combination with its ease of preparation and the low costs if its precursors, open the way to expanding the fields of application for this class of materials, which can also be used in photo- and electrocatalysis, batteries, etc. Research in these fields is currently underway and will be reported in due course.

CRediT authorship contribution statement

Benedetto Taormina: Writing – review & editing, Writing – original draft, Visualization, Investigation, Formal analysis, Data curation. **Francesca Cecchet:** Writing – original draft, Validation, Investigation, Formal analysis, Data curation. **Michelangelo Gruttadauria:** Writing – review & editing, Validation, Supervision. **Carmela Aprile:** Writing – review & editing, Validation, Supervision, Resources, Funding acquisition, Conceptualization. **Francesco Giacalone:** Writing – review & editing, Writing – original draft, Validation, Supervision, Resources, Project administration, Methodology, Funding acquisition, Conceptualization.

Declaration of Competing Interest

The authors declare the following financial interests/personal relationships which may be considered as potential competing interests. Francesco Giacalone reports financial support was provided by Italian Ministry of Education. Carmela Aprile reports financial support was provided by F.R.S-FNRS. Carmela Aprile reports financial support was provided by FEDER. If there are other authors, they declare that they have no known competing financial interests or personal relationships that could have appeared to influence the work reported in this paper.

Acknowledgements

This research was partially funded by University of Palermo and the Italian Ministry of Education (PRIN 2017 project no. 2017W8KNZW). This research is supported by the F.R.S-FNRS via funding grants GEQ U. G014.19 EQP U.N034.17 and PDR T.0004.21, European Regional Development Fund (FEDER). B. T. gratefully acknowledges the University of Palermo and University of Namur for a co-funded PhD fellowship. The authors acknowledge Dr. Luca Fusaro for his support to the NMR experiments. This research used resources of PC2 (Plateforme Technologique Physico-Chemical Characterization), MORPH-IM (Morphology & Imaging), LOS (Lasers, Optics & Spectroscopied) and SIAM (Synthesis, Irradiation & Analysis of Materials) technology platforms located at the University of Namur.

Appendix A. Supporting information

Supplementary data associated with this article can be found in the online version at doi:10.1016/j.jece.2026.121516.

Data availability

Data will be made available on request.

References

[1] A.B.P. Lever, The phthalocyanines—molecules of enduring value; a two-dimensional analysis of redox potentials, J. Porphyr. Phthalocyanines 3 (1999) 488–511, https://doi.org/10.1002/(SICI)1099-1409(199908/10)3:6/7.
[2] A.B. Sorokin, Phthalocyanine metal complexes in catalysis, Chem. Rev. 113 (2013) 8152–8191, https://doi.org/10.1021/cr4000072.
[3] S. Yang, Y. Yu, X. Gao, Z. Zhang, F. Wang, Recent advances in electrocatalysis with phthalocyanines, Chem. Soc. Rev. 50 (2021) 12985–13011, https://doi.org/10.1039/D0CS01605E.
[4] J. Jiang, H. Wang, K. Wang, Application of phthalocyanine in photocatalysis. Phthalocyanine-Based Functional Polymeric Materials: Design, Synthesis, and Applications, Wiley, Hoboken, New Jersey, 2025, pp. 269–312.
[5] Y. Wu, Y. Liang, H. Wang, Heterogeneous molecular catalysts of metal phthalocyanines for electrochemical CO_2 reduction reactions, Acc. Chem. Res. 54 (2021) 3149–3159, https://doi.org/10.1021/acs.accounts.1c00200.
[6] Y. Kim, D. Kim, J. Lee, L.Y.S. Lee, D.K.P. Ng, Tuning the electrochemical properties of polymeric cobalt phthalocyanines for efficient water splitting, Adv. Funct. Mater. 31 (2021) 2103290, https://doi.org/10.1002/adfm.202103290.
[7] S. Keshipour, A. Asghari, A review on hydrogen generation by phthalocyanines, Int. J. Hydrog. Energy 47 (2022) 12865–12881, https://doi.org/10.1016/j.ijhydene.2022.02.058.
[8] Y. Gök, O.T. Arlı, H.Z. Gök, R. Erdem, Preparation of mesoporous silica nanostructure functionalized with hydrobenzoin substituted phthalocyanine and its catalytic performance in benzyl alcohol oxidation, Appl. Organomet. Chem. 39 (2025) e7925, https://doi.org/10.1002/aoc.7925.
[9] F. Zeng, Y. Chen, L. Kan, L. Liu, J. Zhang, G. Tian, Biphase TiO_2/Zn-tetracarboxyphthalocyanine twin S-scheme heterojunction nanowires with efficient charge transfer and CO_2 photocatalytic conversion, Sep. Purif. 356 (2025) 129870, https://doi.org/10.1016/j.seppur.2024.129870.
[10] H. Jia, Y. Yao, J. Zhao, Y. Gao, Z. Luo, P. Du, A novel two-dimensional nickel phthalocyanine-based metal–organic framework for highly efficient water

oxidation catalysis, J. Mater. Chem. A 6 (2018) 1188–1195, https://doi.org/10.1039/C7TA07978H.
[11] G. Bottari, G. de la Torre, T. Torres, Phthalocyanine–nanocarbon ensembles: From discrete molecular and supramolecular systems to hybrid nanomaterials, Acc. Chem. Res. 48 (2015) 900–910, https://doi.org/10.1021/ar5004384.
[12] S. Reich, C. Thomsen, J. Maultzsch, Carbon Nanotubes: Basic Concepts and Physical Properties, Wiley-VCH, Weinheim, 2007.
[13] D.M. Guldi, N. Martín, Carbon Nanotubes and Related Structures: Synthesis, Characterization, Functionalization, and Applications, Wiley-VCH, Weinheim, 2010.
[14] B. Taormina, R. Jouclas, A. Dsouza, A. Morena, M. Gruttadauria, C. Aprile, F. Giacalone, Metal phthalocyanines and imidazolium bromide copolymers supported on multi-walled carbon nanotubes: a "lego-like" assembly of hybrid bifunctional materials applied for CO_2 conversion, Carbon 12050 (2025), https://doi.org/10.1016/j.carbon.2025.120508.
[15] B. Taormina, R. Jouclas, V. Marsala, M. Gruttadauria, F. Giacalone, C. Aprile, Imidazolium bromide substituted magnesium phthalocyanine polymers, N. Promis. Mater. CO_2 Convers. J. CO_2 Util. 85 (2024) 102875, https://doi.org/10.1016/j.jcou.2024.102875.
[16] L. Valentino, V. Campisciano, C. Célis, V. Lemaur, R. Lazzaroni, M. Gruttadauria, C. Aprile, F. Giacalone, Highly cross-linked bifunctional magnesium porphyrin-imidazolium bromide polymer: Unveiling the key role of co-catalysts proximity for CO_2 conversion into cyclic carbonates, J. Catal. 428 (2023) 115143, https://doi.org/10.1016/j.jcat.2023.115143.
[17] V. Campisciano, L. Valentino, A. Morena, A. Santiago-Portillo, N. Saladino, M. Gruttadauria, C. Aprile, F. Giacalone, Carbon nanotube supported aluminum porphyrin-imidazolium bromide crosslinked copolymer, A Synerg. bifunctional Catal. CO_2 Convers. J. CO_2 Util. 57 (2022) 101884, https://doi.org/10.1016/j.jcou.2022.101884.
[18] A. Morena, V. Campisciano, A. Santiago-Portillo, M. Gruttadauria, F. Giacalone, C. Aprile, POSS-Al-porphyrin-imidazolium cross-linked network as catalytic bifunctional platform for the conversion of CO_2 with epoxides, Fuel 336 (2023) 126819, https://doi.org/10.1016/j.fuel.2022.126819.
[19] H.K. Porter, The Zinin reduction of nitroarene. Organic Reactions, Wiley, Hoboken, New Jersey, 2011, pp. 455–481.
[20] H.J. Arpe, Industrial Organic Chemistry, Wiley-VCH, 2010.
[21] B. Amini, S. Lowenkron, Kirk-Othmer Encyclopedia of Chemical Technology, John Wiley & Sons, Inc, Hoboken, New Jersey, 2003, p. 783.
[22] D. Formenti, F. Ferretti, F.K. Scharnagl, M. Beller, Reduction of nitro compounds using 3d-non-noble metal catalysts, Chem. Rev. 119 (2019) 2611–2680, https://doi.org/10.1021/acs.chemrev.8b00547.
[23] M. Wang, K. Ishii, Photochemical properties of phthalocyanines with transition metal ions, Coord. Chem. Rev. 468 (2022) 214626, https://doi.org/10.1016/j.ccr.2022.214626.
[24] A. Ahmad, R.A. Collins, FTIR characterization of triclinic lead phthalocyanine, J. Phys. D Appl. Phys. 24 (1991) 1894–1897, https://doi.org/10.1088/0022-3727/24/10/029.
[25] M.M. El-Nahass, A.M. Farid, A.A. Attia, H.A.M. Ali, Structural properties and UV to NIR absorption spectra of metal-free phthalocyanine (H_2PC) thin films, Fiz. A (Zagreb) 15 (2006) 147–164.
[26] R. Seoudi, G.S. El-Bahy, Z.A. El-Sayed, FTIR, TGA and DC electrical conductivity studies of phthalocyanine and its complexes, J. Mol. Struct. 753 (2005) 119–126, https://doi.org/10.1016/j.molstruc.2005.06.003.
[27] M.M. El-Nahass, K.F. Abd-El-Rahman, A.A.A. Darwish, Fourier-transform infrared and UV–vis spectroscopes of nickel phthalocyanine thin films, Mater. Chem. Phys. 92 (2005) 185–189, https://doi.org/10.1016/j.matchemphys.2005.01.008.
[28] T. Kobayashi, F. Kurokawa, N. Uyeda, E. Suito, The metal-ligand vibrations in the infrared spectra of various metal phthalocyanines, Spectrochim. Acta A Mol. Biomol. Spectrosc. 26 (1970) 1305–1311, https://doi.org/10.1016/0584-8539(70)80036-8.
[29] Thermo Fisher Scientific (2025) Iron. Materials Science Learning Center. ⟨https://www.thermofisher.com/be/en/home/materials-science/learning-center/periodic-table/transition-metal/iron.html⟩. Accessed 7 April 2025.
[30] Z. Li, L. Deng, I.A. Kinloch, R.J. Young, Raman spectroscopy of carbon materials and their composites: graphene, nanotubes and fibres, Prog. Mater. Sci. 135 (2023) 101089, https://doi.org/10.1016/j.pmatsci.2023.101089.
[31] V. Campisciano, C. Calabrese, L.F. Liotta, V. La Parola, A. Spinella, C. Aprile, et al., Templating effect of carbon nanoforms on highly cross-linked imidazolium network: catalytic activity of the resulting hybrids with Pd nanoparticles, Appl. Organomet. Chem. 33 (2019) e4848, https://doi.org/10.1002/aoc.4848.
[32] V. Campisciano, R. Burger, C. Calabrese, L.F. Liotta, P.L. Lo Meo, M. Gruttadauria, F. Giacalone, Straightforward preparation of highly loaded MWCNT–polyamine hybrids and their application in catalysis, Nanoscale Adv. 2 (2020) 4199–4211, https://doi.org/10.1039/d0na00291g.
[33] A. Morena, V. Campisciano, A. Comès, L.F. Liotta, M. Gruttadauria, C. Aprile, F. Giacalone, A study on the stability of carbon nanoforms–polyimidazolium network hybrids in the conversion of CO_2 into cyclic carbonates: Increase in catalytic activity after reuse, Nanomaterials 11 (2021) 2243, https://doi.org/10.3390/nano11092243.
[34] I. Ziccarelli, R. Mancuso, F. Giacalone, C. Calabrese, V. La Parola, A. de Salvo, N. Della Ca', M. Gruttadauria, B. Gabriele, Heterogenizing palladium tetraiodide catalyst for carbonylation reactions, J. Catal. 413 (2022) 1098–1110, https://doi.org/10.1016/j.jcat.2022.08.007.
[35] L. Valentino, R. Di Forti, A. Morena, C. Aprile, M. Gruttadauria, F. Giacalone, V. Campisciano, Polymerizable deep eutectic solvents: convenient reactive dispersion media for the preparation of novel multi-walled carbon nanotubes-based functional materials, Chem. Eng. J. 489 (2024) 151447, https://doi.org/10.1016/j.cej.2024.151447.
[36] M. Borjian Boroujeni, M.S. Laeini, M.T. Nazeri, A. Shaabani, A novel and green in situ strategy for the synthesis of metallophthalocyanines on chitosan and investigation their catalytic activity in the CO_2 fixation, Catal. Lett. 149 (2019) 2089–2097, https://doi.org/10.1007/s10562-019-02740-8.
[37] A.C.S. Gonzalez, A.P. Felgueiras, R.T. Aroso, R.M.B. Carrilho, M.M. Pereira, Al(III) phthalocyanine catalysts for CO_2 addition to epoxides: fine-tunable selectivity for cyclic carbonates versus polycarbonates, J. Organomet. Chem. 950 (2021) 121979, https://doi.org/10.1016/j.jorganchem.2021.121979.
[38] T. Zhang, X. Wang, X. Huang, Y. Liao, J. Chen, Bifunctional catalyst of a metallophthalocyanine–carbon nitride hybrid for chemical fixation of CO_2 to cyclic carbonate, RSC Adv. 6 (2016) 2810–2818, https://doi.org/10.1039/C5RA2105.
[39] E.M. Maya, A. Valverde-González, M. Iglesias, Conversion of CO_2 into chloropropene carbonate catalyzed by iron (II) phthalocyanine hypercrosslinked porous organic polymer, Molecules 25 (2020) 4598, https://doi.org/10.3390/molecules25204598.
[40] T. Nasiriani, M.T. Nazeri, A. Shaabani, Cobalt phthalocyanine conjugated SBA-15 mesoporous silica via the Ugi four-component reaction: a potential heterogeneous catalytic nanocomposite for CO2 fixation reaction, Micro Mesopor. Mater. 354 (2023) 112514, https://doi.org/10.1016/j.micromeso.2023.112514.
[41] M.T. Nazeri, S. Javanbakht, M. Ramezani, A. Shaabani, A facile and green synthesis of cobalt phthalocyanine-conjugated multiwall carbon nanotube by the Ugi reaction: an efficient CO_2 fixation catalyst, J. Taiwan Inst. Chem. Eng. 136 (2022) 104428, https://doi.org/10.1016/j.jtice.2022.104428.
[42] T. Kessaratikoon, T. Theerathanagorn, D. Crespy, V. D'Elia, Organocatalytic polymers from affordable and readily available building blocks for the cycloaddition of CO2 to epoxides, J. Org. Chem. 88 (2023) 4894–4924, https://doi.org/10.1021/acs.joc.2c02447.
[43] P. Tyagi, D. Singh, N. Malik, S. Kumar, R. Singh Malik, Metal catalyst for CO2 capture and conversion into cyclic carbonate: progress and challenges, Mater. Today 65 (2023) 133–165, https://doi.org/10.1016/j.mattod.2023.02.029.
[44] R. Luo, M. Chen, X. Liu, W. Xu, J. Li, B. Liu, Y. Fang, Recent advances in CO2 capture and simultaneous conversion into cyclic carbonates over porous organic polymers having accessible metal sites, J. Mater. Chem. A 8 (2020) 18408–18424, https://doi.org/10.1039/D0TA06142E.
[45] Z. Su, L. Ma, J. Wei, X. Bai, N. Wang, J. Li, A zinc porphyrin polymer as efficient bifunctional catalyst for conversion of CO2 to cyclic carbonates, Appl. Organomet. Chem. 36 (2022) e6632, https://doi.org/10.1002/aoc.6632.
[46] J. Liu, G. Zhao, O. Cheung, L. Jia, Z. Sun, S. Zhang, Highly porous metalloporphyrin covalent ionic frameworks with well-defined cooperative functional groups as excellent catalysts CO2 cycloaddition, Chem. Eur. J. 25 (2019) 9052–9059, https://doi.org/10.1002/chem.201900992.
[47] D. Reay, C. Ramshaw, A. Harvey, Chapter 1 - A Brief History of Process Intensification, in: D. Reay, C. Ramshaw, A. Harvey (Eds.), Process Intensification, second Ed, Butterworth-Heinemann, Oxford, 2013, pp. 1–25.
[48] J.P. Lange, US Patent 7728164B2 (2010) to Shell Oil Company.
[49] P.K. Verma, M. Bala, K. Thakur, U. Sharma, N. Kumar, B. Singh, Iron and palladium (II) phthalocyanines as recyclable catalysts for reduction of nitroarenes, Catal. Lett. 144 (2014) 1258–1267, https://doi.org/10.1007/s10562-014-1269-6.
[50] U. Sharma, P. Kumar, N. Kumar, V. Kumar, B. Singh, Highly chemo- and regioselective reduction of aromatic nitro compounds catalyzed by recyclable copper(II) as well as cobalt(II) phthalocyanines, Adv. Synth. Catal. 352 (2010) 1834–1840, https://doi.org/10.1002/adsc.201000191.
[51] C.G. Chao, D.E. Bergbreiter, Highly organic phase soluble polyisobutylene-bound cobalt phthalocyanines as recyclable catalysts for nitroarene reduction, Catal. Commun. 77 (2016) 89–93.
[52] U. Sharma, N. Kumar, P.K. Verma, V. Kumar, B. Singh, Zinc phthalocyanine with PEG-400 as a recyclable catalytic system for selective reduction of aromatic nitro compounds, Green. Chem. 14 (2012) 2289–2293, https://doi.org/10.1039/C2GC35452G.
[53] T. Aditya, A. Pal, T. Pal, Nitroarene reduction: a trusted model reaction to test nanoparticle catalysts, Chem. Commun. 51 (46) (2015) 9410–9431, https://doi.org/10.1039/C5CC01131K.
[54] P. Lara, K. Philippot, The hydrogenation of nitroarenes mediated by platinum nanoparticles: an overview, Catal. Sci. Technol. 4 (2014) 2445–2465, https://doi.org/10.1039/C4CY00111G.
[55] H.K. Kadam, S.G. Tilve, Advancement in methodologies for reduction of nitroarenes, RSC Adv. 5 (2015) 83391–83407, https://doi.org/10.1039/C5RA10076C.
[56] D. Formenti, F. Ferretti, F.K. Scharnagl, M. Beller, Reduction of nitro compounds using 3d-non-noble metal catalysts, Chem. Rev. 119 (2019) 2611–2680, https://doi.org/10.1021/acs.chemrev.8b00547.